

**Aerosol optical and  
microphysical  
retrievals from  
a hybrid lidar dataset**

P. Sawamura et al.

**Aerosol optical and microphysical  
retrievals from a hybrid multiwavelength  
lidar dataset – DISCOVER-AQ 2011**

**P. Sawamura<sup>1,5,\*</sup>, D. Müller<sup>3</sup>, R. M. Hoff<sup>2</sup>, C. A. Hostetler<sup>1</sup>, R. A. Ferrare<sup>1</sup>,  
J. W. Hair<sup>1</sup>, R. R. Rogers<sup>1</sup>, B. E. Anderson<sup>1</sup>, L. D. Ziemba<sup>1</sup>, A. J. Beyersdorf<sup>1</sup>,  
K. L. Thornhill<sup>1</sup>, E. L. Winstead<sup>1</sup>, and B. N. Holben<sup>4</sup>**

<sup>1</sup>NASA Langley Research Center, Hampton, VA 23681, USA

<sup>2</sup>University of Maryland, Baltimore County, Baltimore, MD 21250, USA

<sup>3</sup>University of Hertfordshire, College Lane, Hatfield, Herts, AL 10 9AB, UK

<sup>4</sup>NASA Goddard Space Flight Center, Greenbelt, MD 20771, USA

<sup>5</sup>Oak Ridge Associated Universities (ORAU), TN 37831, USA

\*formerly at: University of Maryland, Baltimore County, Baltimore, MD 21250, USA

Received: 20 February 2014 – Accepted: 7 March 2014 – Published: 28 March 2014

Correspondence to: P. Sawamura (patricia.sawamura@nasa.gov)

Published by Copernicus Publications on behalf of the European Geosciences Union.

Title Page

Abstract

Introduction

Conclusions

References

Tables

Figures

⏪

⏩

◀

▶

Back

Close

Full Screen / Esc

Printer-friendly Version

Interactive Discussion

## Abstract

Retrievals of aerosol microphysical properties (e.g. effective radius, volume and surface-area concentrations) and aerosol optical properties (e.g. complex index of refraction and single scattering albedo) were obtained from a hybrid multiwavelength lidar dataset for the first time. In July of 2011, in the Baltimore-Washington DC region, synergistic profiling of optical and microphysical properties of aerosols with both airborne in-situ and ground-based remote sensing systems was performed during the first deployment of DISCOVER-AQ. The hybrid multiwavelength lidar dataset combines elastic ground-based measurements at 355 nm with airborne High Spectral Resolution Lidar (HSRL) measurements at 532 nm and elastic measurements at 1064 nm that were obtained less than 5 km apart of each other. This was the first study in which optical and microphysical retrievals from lidar were obtained during the day and directly compared to AERONET and in-situ measurements for 11 cases. Good agreement was observed between lidar and AERONET retrievals. Larger discrepancies were observed between lidar retrievals and in-situ measurements obtained by the aircraft and aerosol hygroscopic effects are believed to be the main factor of such discrepancies.

## 1 Introduction

Aerosols are known to play an important role in chemical processes, cloud formation, air quality, radiative balance, among other atmospheric processes. In the last few decades great progress has been achieved towards a better understanding of the optical and physical properties of aerosols, and also on how changes in those properties affect the atmospheric radiative processes. Currently, many instruments onboard satellites allow for retrievals of column-integrated properties of aerosols on a daily basis. In addition to satellites, a number of ground-based networks contribute with continuous aerosol observations. However, despite this continuous advance, it is indisputable that many gaps in our understanding of aerosols are yet to be filled.

## Aerosol optical and microphysical retrievals from a hybrid lidar dataset

P. Sawamura et al.

Title Page

Abstract

Introduction

Conclusions

References

Tables

Figures

◀

▶

◀

▶

Back

Close

Full Screen / Esc

Printer-friendly Version

Interactive Discussion



## Aerosol optical and microphysical retrievals from a hybrid lidar dataset

P. Sawamura et al.

Title Page

Abstract

Introduction

Conclusions

References

Tables

Figures

◀

▶

◀

▶

Back

Close

Full Screen / Esc

Printer-friendly Version

Interactive Discussion

Aerosols originate both naturally and from anthropogenic processes. Globally, more than half of all particle emissions are of anthropogenic origin (Jacobson, 2012). These particles enter the atmosphere through emissions and nucleation. While suspended in the atmosphere the sizes of these particles as well as their number distributions evolve as they undergo coagulation, condensation, water uptake, chemical reactions, and removal processes.

The sizes and types of aerosols can be display large variations both in spatial and temporal scale. Therefore, a continuous effort to monitor the particles present in the boundary layer is necessary.

An important aspect on how these particles affect our climate is that the radiative forcing due to aerosols depends on their vertical distribution. For instance, due to hygroscopic growth effects, scattering particles produce a greater forcing when the majority of aerosol particles are located in the lower troposphere, whereas absorbing particles will produce a greater forcing above clouds/cloudy layers or when the underlying surface albedo is high (Haywood and Ramaswamy, 1998). Also, surface temperature and climate responses depend on both vertical and horizontal distribution of aerosols (Hansen et al., 1997). And for that reason, a proper characterization of the vertical distribution of aerosols is necessary.

## 2 Motivation

Retrievals based on the inversion of multi-spectral radiance measurements obtained by ground based and spaceborne radiometers are representative of the entire atmospheric column and therefore do not provide information on how the aerosols are distributed throughout the column. Lidars, on the other hand, are capable of determining the vertical distribution of aerosols with high spatial and temporal resolution. Many ground-based lidar networks across the globe such as the European Lidar Network (EARLINET: Bösenberg et al., 2003), the Micropulse Lidar Network (MPLNET: Welton

et al., 2001), and the Asian Dust Network (ADNet: Sugimoto and Uno, 2009) contribute to regular aerosol observations.

Over the past decade, the development of inversion techniques for the retrieval of microphysical properties (such as effective radius, number, surface-area and volume concentrations) and optical parameters (such as absorption and scattering coefficients, single scattering albedo and complex index of refraction) from multiwavelength lidar systems brought a new perspective in the study of the vertical distribution of aerosols (Müller et al., 1998, 1999a, b). In contrast to most radiometers (e.g. from MODIS and AERONET) which measure radiance over a large number of wavelengths, it has been demonstrated that from lidar backscatter and extinction measurements at three wavelengths, one can obtain retrievals of the aforementioned aerosol optical and physical properties.

More specifically, the recommended multiwavelength lidar dataset necessary to obtain such retrievals consists of a set of backscatter coefficients ( $\beta$ ) at 355 nm, 532 nm and 1064 nm and a set of extinction coefficients ( $\alpha$ ) at 355 nm and 532 nm (Veselovskii et al., 2002; Bockmann et al., 2005), which are the usual wavelength outputs from a Nd:YAG laser.

All microphysical retrievals from multiwavelength lidar data obtained to date, however, originated from ground-based Raman lidar systems which have one major drawback: Raman lidars are generally limited to nighttime operations due to the weak Raman backscattering signal which makes it very sensitive to solar background radiation. Therefore it can be very difficult to characterize the aerosol variation throughout the day with Raman lidar systems. Wandinger et al. (2002) compared nighttime lidar retrievals of effective radius, volume and surface-area concentrations, complex index of refraction and single-scattering albedo with nighttime airborne in-situ measurements for two cases and obtained good agreement during LACE 98. In this study good agreement (< 30%) was obtained between the lidar retrievals and the in-situ measurements for cases of aerosols originated from forest fires. Veselovskii et al. (2009) compared early nighttime retrievals of mean and effective radius, angstrom coefficient,

## Aerosol optical and microphysical retrievals from a hybrid lidar dataset

P. Sawamura et al.

Title Page

Abstract

Introduction

Conclusions

References

Tables

Figures

⏪

⏩

◀

▶

Back

Close

Full Screen / Esc

Printer-friendly Version

Interactive Discussion





## Aerosol optical and microphysical retrievals from a hybrid lidar dataset

P. Sawamura et al.

Title Page

Abstract

Introduction

Conclusions

References

Tables

Figures

◀

▶

◀

▶

Back

Close

Full Screen / Esc

Printer-friendly Version

Interactive Discussion

from Column and Vertically Resolved Observations Relevant to Air Quality) is a five-year field experiment funded by the NASA Earth Venture program. The goal of DISCOVER-AQ is to improve our understanding on how to relate total-column observations with near-surface conditions of aerosol and trace gases (Hoff et al., 2012; DISCOVER-AQ, 2011).

During this campaign a number of ground-based and airborne instruments were deployed throughout the Baltimore-Washington DC region providing the data necessary to construct the hybrid multiwavelength lidar dataset. Optical and physical parameters of aerosols from airborne in-situ instruments as well as from ground-based sunphotometers were also obtained during this experiment and compared with our lidar retrievals. Figure 1 shows a map with the locations of interest during this study.

The hybrid lidar dataset as well as the inversion methodology are described in more detail in Sect. 3. Discussion of results and comparison of the lidar retrievals with airborne in-situ measurements as well as with AERONET inversion products are presented in Sect. 4.

### 3 Methodology

#### 3.1 Hybrid multiwavelength lidar dataset

In order to obtain retrievals of the optical and microphysical properties of aerosols from a multiwavelength lidar system, a minimum set of backscatter and extinction coefficient measurements is required as demonstrated by Veselovskii et al. (2004) and Bockmann et al. (2005). As previously mentioned, most studies and efforts in characterizing the optical and microphysical properties of tropospheric aerosols through the inversion of multiwavelength lidar data have taken place in either Europe or Asia. Furthermore, most of those studies utilized Raman lidar systems that were specifically designed for multiwavelength measurements. These instruments were designed to emit and receive photons of all three wavelengths at the same time and through the same optical path

allowing for completely collocated measurements, and therefore a more self-consistent  $3\beta + 2\alpha$  dataset.

Compared to a few years ago, the availability of multiwavelength lidar systems has increased. But still, most of those systems are operated by the European Aerosol Lidar Research Network (EARLINET). Many lidar groups across the globe still operate instruments that are not capable of providing a complete  $3\beta + 2\alpha$  dataset.

As an alternative to the  $3\beta + 2\alpha$  inversion methodology, some studies were carried out also in the framework of EARLINET in which backscatter and extinction coefficients obtained from a Raman lidar were combined with optical depth measured by sunphotometer in order to derive the microphysical properties of aerosols (Pahlow et al., 2006; Tesche et al., 2008). Wagner et al. (2013) combined backscatter and extinction coefficients obtained from a Raman lidar and retrievals of volume concentration and column values of the volume-specific backscatter and extinction values obtained from AERONET in an optimization algorithm in order to obtain vertically resolved distributions of optical and microphysical properties of fine and coarse mode particles. However, the main challenge that comes to mind in this type of Raman lidar and AERONET data combination is temporal data collocation. Sunphotometers are fundamentally designed to be operated during daytime while Raman lidars allow for good measurements mostly during nighttime.

The objective of this work was to explore the feasibility of applying the  $3\beta + 2\alpha$  inversion methodology to a hybrid multiwavelength lidar dataset in order to expand the aerosol microphysical characterization efforts beyond what has been done so far.

During DISCOVER-AQ, the NASA UC-12 aircraft flew across the Baltimore-Washington DC region with the HSRL-1 system on board obtaining profiles of extinction and backscatter coefficients at 532 utilizing the HSRL technique as well as profiles of backscatter coefficient at 1064 with the elastic technique (Hair et al., 2008). Measurements of depolarization ratio at 532 nm and 1064 nm were also obtained simultaneously with the HSRL-1 system. Profiles of backscatter and extinction coefficient at

## Aerosol optical and microphysical retrievals from a hybrid lidar dataset

P. Sawamura et al.

Title Page

Abstract

Introduction

Conclusions

References

Tables

Figures



Back

Close

Full Screen / Esc

Printer-friendly Version

Interactive Discussion

355 nm were obtained at the University of Maryland, Baltimore County (UMBC) using a commercial ground-based elastic lidar (Leosphere, ALS-450).

In order to combine the dual-platform lidar measurements (e.g., airborne and ground-based), a collocation radius of 5 km centered at the Department of Physics at UMBC (39.25°, -76.71°) was considered. Figure 2 depicts the setup. Within this radius it is assumed that the airmass is homogeneous enough so that measurements from different instruments can be combined, and we examine this assumption.

The hybrid dataset not only combines dual-platform measurements, but it also combines both elastic and high spectral resolution lidar techniques which can be a challenging task.

The HSRL is a more robust technique when compared to the standard elastic lidar technique since it utilizes spectral delineation to separate the signal contribution due to aerosol and molecules which allows for the determination of both backscatter and extinction coefficients independently. Elastic lidar systems, however, measure the total attenuated backscatter due to molecules and aerosols together. For this type of system, the extinction coefficient is retrieved with the assumption of a constant extinction-to-backscatter ratio (i.e. lidar ratio). The lidar ratio, as an intensive property, varies with the type of aerosol. Therefore, the assumption of a constant lidar ratio throughout the whole column of the atmosphere can be problematic in cases when layers of different types of aerosols are present. In order to assess the feasibility of this new retrieval methodology, we tested the 5 km airmass homogeneity assumption as well as the constant lidar ratio assumption. This is discussed in the next section.

### 3.1.1 Elastic lidar retrievals

During this experiment, in addition to the airborne HSRL-1 system and the ALS-450, another elastic lidar obtained measurements at 532 nm at UMBC (ELF: Elastic Lidar Facility).

The Leosphere ALS-450 is a commercial, eye-safe elastic lidar system that utilizes a tripled pulse laser source Nd:YAG at 355 nm at 20 Hz repetition rate generating

## Aerosol optical and microphysical retrievals from a hybrid lidar dataset

P. Sawamura et al.

Title Page

Abstract

Introduction

Conclusions

References

Tables

Figures

⏪

⏩

◀

▶

Back

Close

Full Screen / Esc

Printer-friendly Version

Interactive Discussion



## Aerosol optical and microphysical retrievals from a hybrid lidar dataset

P. Sawamura et al.

Title Page

Abstract

Introduction

Conclusions

References

Tables

Figures

⏪

⏩

◀

▶

Back

Close

Full Screen / Esc

Printer-friendly Version

Interactive Discussion

measurements with temporal and spatial resolution of 1 min and 15 m, respectively. ELF utilizes a Q-switched Continuum Surelite II Nd:YAG operating at 1064 nm and 532 nm with a 10 Hz repetition rate. ELF's signal is digitized with a Licel TR20-160 photon counter and averaged for one minute, with a vertical resolution of 7.5 m. More details on ELF system can be found elsewhere (Comer, 2003; Engel-Cox et al., 2006). The technical specifications of the HSRL system can be found in details in Hair et al. (2008).

Both elastic systems utilize similar algorithms to retrieve the extinction coefficient from the total attenuated backscatter signal which relies on closing the integrated extinction profile to aerosol optical depth (AOD) measurements obtained by a collocated AERONET sunphotometer. Having an elastic lidar at 532 nm at the same location as the ALS-450 enabled us to assess the two aforementioned assumptions at the same time by comparing the extinction coefficient profiles from ELF and from HSRL-1 using the same spatial subset proposed (i.e.  $r < 5$  km). Figure 3 shows the profiles comparison for all cases analyzed in this work (itemized in Table 1) which shows sufficient agreement. The error bars (shaded area) in the HSRL profile are the standard deviation of the profiles during an UMBC overpass which usually lasted between 1 and 2 min, resulting in a 5–10 profile average. The errors in ELF profiles are the standard deviation of 15 profiles which represent a 15 min average centered at the UMBC overpass by the UC-12. The agreement observed between HSRL and ELF profiles was a good indicator of the feasibility of combining dual-platform, dual-technique lidar data to perform the retrievals. For the cases in hand the aerosol intensive properties do not show much variation with altitude, therefore the assumption of a constant lidar ratio throughout the atmosphere is reasonable. The agreement between both profiles also indicates that the assumption of a homogeneous air mass within 5 km and/or 15 min is reasonable as well. In Fig. 3 we also show the extinction profiles obtained from in-situ measurements onboard the P3B over the closest spiral sites. Good agreement can be observed in most cases which corroborates and also extends the air mass horizontal homogeneity assumption to larger distances (Padonia and Beltsville sites were about

22 km from UMBC and Essex about 10 km). The discrepancies observed in other cases were mostly in isolated layers aloft where the homogeneity assumption fails.

The method utilized to obtain the aerosol extinction and backscatter profiles for both elastic lidar systems is an iterative algorithm that selects the optimum lidar ratio value by minimizing the residual between the AERONET AOD and the lidar AOD calculated from the integrated extinction coefficient profile. Some small differences in the algorithm utilized for ELF and the ALS-450 should be noted. ELF's algorithm utilizes AOD measurements of an entire day in the residue minimization process thus resulting in a single value of lidar ratio for that particular day. The algorithm utilized with the ALS-450 dataset, however, was run in a case-by-case scenario obtaining a lidar ratio value for each case. Figure 4 shows the so-called  $3\beta + 2\alpha$  dataset as well as the lidar ratio values at 355 and 532 nm obtained from both HSRL-1 and ALS-450. The error bars in the profiles at 355 nm were obtained by varying the system constant in the lidar equation by 5% and then averaging the lidar ratio values obtained and the corresponding profiles. In a couple of cases, like seen in plots B and C from Fig. 4, the algorithm found a larger number of acceptable lidar ratio values but it did not, however, translate to a large variation in the backscatter and extinction profiles.

### 3.1.2 Lidar inversion algorithm for retrieval of microphysical and optical properties of aerosols

The idea of retrieving aerosol size distributions from multiwavelength lidar measurements started back in the 1980s, with Heintzenberg and Qing offering two different approaches (Heintzenberg et al., 1981; Qing et al., 1989). Based on the work of Qing et al. (1989) this topic was revitalized in the mid 1990s, culminating in the late 1990s in the first version of an inversion algorithm to retrieve aerosol microphysical properties from multiwavelength lidar data that consist of a combination of particle backscatter and extinction coefficients measured at multiple wavelengths (Müller et al., 1998). Since then, many studies have been carried out showing that measurements of combined backscatter and extinction coefficients allow indeed for the retrieval of aerosol size

## Aerosol optical and microphysical retrievals from a hybrid lidar dataset

P. Sawamura et al.

Title Page

Abstract

Introduction

Conclusions

References

Tables

Figures

◀

▶

◀

▶

Back

Close

Full Screen / Esc

Printer-friendly Version

Interactive Discussion



distributions parameters with reasonable accuracy (Müller et al., 1999a; Veselovskii et al., 2002; Bockmann et al., 2005).

The first retrievals from lidar data were derived with the inversion method described by Müller et al. (1998, 1999a, b, 2000). This method was specifically developed to process optical data from an eleven-channel, six-wavelengths scanning Raman lidar system (Althausen et al., 2000). Since then, the algorithm was further refined to handle more limited datasets, dubbed  $3\beta + 2\alpha$  (or simply  $3 + 2$ ) (Müller et al., 2001; Veselovskii et al., 2002; Bockmann et al., 2005). The  $3\beta + 2\alpha$  dataset is the minimum requirement for the retrieval of microphysical particle properties with the current inversion algorithm.

The problem of retrieving intrinsic physical characteristics of aerosols from a limited set of optical measurements is known to be an ill-posed problem in inversion theory. In summary, the algorithm relies on the relationship of the spectral optical data (i.e. extinction and backscatter coefficients) to the physical characteristics of *spherical* aerosols (i.e. size and complex index of refraction) through kernel functions that are related to the extinction and backscatter efficiencies described by Mie theory (Mie, 1908; Bohren and Huffman, 1983). In order to solve the equations, which can be found in the literature referenced herein, the size distribution is discretized and approximated by a linear combination of triangular-shaped B-spline functions. The ill-posedness of the problem arises when solving the matrix equations for the weight factors of the linear combination of those triangular functions. In this case regularization methods must be introduced because the simple solution of such equation results in error amplification and discontinuity of solutions due to the ill-posedness of the mathematical problem. The procedure aims at stabilizing the solution space by introducing mathematical and physical constraints during the inversion process, as well as after the inversion process during post-processing.

The current inversion algorithm employs non-descriptive methods, meaning that they do not require any a priori information. It utilizes a minimization concept, also known as method of minimum distance (Tikhonov and Arsenin, 1977; Twomey, 1977), to find the solutions. In simple terms, this method selects solutions for which the residual between

## Aerosol optical and microphysical retrievals from a hybrid lidar dataset

P. Sawamura et al.

Title Page

Abstract

Introduction

Conclusions

References

Tables

Figures

⏪

⏩

◀

▶

Back

Close

Full Screen / Esc

Printer-friendly Version

Interactive Discussion

the solution of the forward problem and the back-calculated solution obtained from the inversion results is smaller than a pre-determined value  $> 0$ . A smoothness constraint is also applied for the size distribution.

In order to obtain the “optimum” smoothness of the size distribution one must find an optimum value for a variable called Lagrange multiplier  $\gamma$ . In the original version of the inversion algorithm, the generalized cross validation (GCV) was utilized to find this optimum  $\gamma$ . Currently, the algorithm employs a modified minimum discrepancy method described by Veselovskii et al. (2002). The mathematical details of this method can be found in Müller et al. (1999a), Twomey (1977) and Weitkamp (2005).

As the inversion problem must be discretized, one must utilize a so-called inversion window which determines the size and complex index of refraction range in which the inversion will take place. The inversion window utilized in this work was  $R_{\min} = 0.01 \mu\text{m} : 0.01 \mu\text{m} : 0.2 \mu\text{m}$ ,  $R_{\max} = 0.5 \mu\text{m} : 0.5 \mu\text{m} : 5 \mu\text{m}$ ,  $\text{Re}[m] = 1.325 : 0.025 : 1.5$ , and  $\text{Im}[m] = 0 : 0.001 : 0.03$ .  $R_{\min}$  and  $R_{\max}$  represent the values for the left and right-most edge of the size distribution, respectively.  $\text{Re}[m]$  and  $\text{Im}[m]$  are the real and imaginary parts of the complex index of refraction ( $m$ ), respectively. The algorithm assumes a wavelength-independent  $m$ . A look-up table of kernel functions is utilized to speed the calculations during the inversion process. The  $R_{\max}$  window was limited to the  $R_{\max}$  range of the kernel functions in this look-up table.

The inversion procedure was run 7 times for each layer. In 6 of those runs, random errors of up to 15% were added to the  $3\beta + 2\alpha$  input set while the remaining run did not have any noise added. This random error is included to account for errors in the measurements. Each inversion run generates a space solution which has to be further constrained in the post-processing step which is the most time consuming part of the process. The constraints are different combinations of  $R_{\min}$ ,  $R_{\max}$  and other regularization parameters that are set manually, making it a very time-consuming task. For each of those 7 solution spaces generated, 5 to 10 post-processing constraints are chosen based on a number of criteria which includes: number of final solutions, physically meaningful complex index of refraction values, and shape of size distribution.

## Aerosol optical and microphysical retrievals from a hybrid lidar dataset

P. Sawamura et al.

Title Page

Abstract

Introduction

Conclusions

References

Tables

Figures

⏪

⏩

◀

▶

Back

Close

Full Screen / Esc

Printer-friendly Version

Interactive Discussion









**Aerosol optical and  
microphysical  
retrievals from  
a hybrid lidar dataset**

P. Sawamura et al.

Title Page

Abstract

Introduction

Conclusions

References

Tables

Figures

⏪

⏩

◀

▶

Back

Close

Full Screen / Esc

Printer-friendly Version

Interactive Discussion



The AERONET volume particle size distributions are retrieved in 22 logarithmically equidistant bins in the radius range size of  $0.05\ \mu\text{m} \leq r \leq 15\ \mu\text{m}$ . The ranges of retrievable real and imaginary parts of the  $m$  are  $1.33 \leq \text{Re}[m] \leq 1.6$  and  $0.0005 \leq \text{Im}[m] \leq 0.5$ , respectively. Details on the algorithms can be found in Dubovik and King (2000) and Dubovik et al. (2000).

Only the fine mode retrievals were considered in the comparison. Also, as the retrievals are obtained for the total column of the atmosphere, the volume particle size distribution is retrieved per unit area ( $\mu\text{m}^3\ \text{cm}^{-2}$ ) instead of per unit volume ( $\mu\text{m}^3\ \text{cm}^{-3}$ ). In order to compare AERONET to lidar retrievals it is necessary to introduce an “aerosol layer height” (ALH) that represents the altitude below which most aerosol particles are confined. For this study, based on the lidar data analyzed we chose  $\text{ALH} = 1.5\ \text{km}$ .

With respect to data quality, AERONET releases its aerosol products as Level 1.5 and 2.0. A number of criteria must be met for the retrievals to be accepted as Level 1.5 and then Level 2.0. These criteria are presented in detail by Holben et al. (2006). In particular,  $\omega_0$  and  $m$  are only “quality assured” (Level 2.0) when AOD at 440 is greater or equal to 0.40 (Dubovik et al., 2000). Due to the large number of criteria utilized to screen the data, Level 2 data during the period analyzed in this study is very scarce. Therefore for the comparison with lidar retrievals we utilized both Level 1.5 and Level 2.0. It should be noted that size-related parameters (i.e. effective radius and volume and surface-area concentrations) usually contains more Level 2 data compared to optical-related parameters (i.e. single-scattering albedo and complex index of refraction).

DRAGON sunphotometers were pre- and post-calibrated for DISCOVER-AQ 2011 and the data goes through the same quality control and quality assurance as the data obtained by the regular AERONET instruments. However we learned later in this study that some DRAGON stations, like Padonia, had possible instrumental issues. Level 2.0 AERONET data was not available for Padonia station. Thus, the comparisons presented in this study with respect to this particular station should be carefully considered.



**Aerosol optical and  
microphysical  
retrievals from  
a hybrid lidar dataset**

P. Sawamura et al.

Title Page

Abstract

Introduction

Conclusions

References

Tables

Figures

◀

▶

◀

▶

Back

Close

Full Screen / Esc

Printer-friendly Version

Interactive Discussion



Table 3 shows the difference in mean effective radius values for the month of July for each AERONET/DRAGON stations considered in this study for three distinct ranges of aerosol optical depth at 440 nm. The differences between Level 1.5 and Level 2.0 for effective radius never exceed 0.01  $\mu\text{m}$  except for Padonia station which does not have Level 2.0 data. However, when compared the other stations, the Level 1.5 effective radius retrieved for Padonia is also within 0.01  $\mu\text{m}$  from both Level 1.5 and Level 2.0 retrievals obtained at the other stations.

Table 4 shows the same comparison as Table 3 but for single-scattering albedo. Here we can clearly see the negative bias in the Level 1.5  $\omega_0$  values obtained for  $\tau_{440} \leq 0.4$  for UMBC and Padonia stations. Level 2.0 data at UMBC is about 0.03 lower compared to Beltsville, Essex and GSFC stations. Padonia Level 1.5 average retrieval for  $\tau_{440} \geq 0.4$  agrees well with both Level 1.5 and 2.0 retrievals from Beltsville, Essex and GSFC stations.

### 4.3 Size parameters

A systematic bias was observed between the lidar retrievals and in-situ measurements of volume and surface-area concentrations.

Compared to lidar retrievals, P-3B measurements showed an average underestimation of about 81 % and 77 % for volume and surface-area concentrations, respectively. The effective radius showed a lower bias of 21 %. The shape of the profiles, however, were in good agreement.

It should be noted that size distribution data from the UHSAS are typically reported referenced to calibrations using polystyrene latex sphere (PSL) particles with a refractive index of 1.59. Because the UHSAS employs an optical detection scheme, sizing (and thus the derived surface area, volume, and effective radius) is sensitive to changes in the real-part of the particle refractive index. In order to better compare to realistic particle compositions which were mixtures of organic compounds and ammonium sulfate (AS), data were corrected using monodisperse AS calibration aerosol (refractive index of 1.53). Resulting correction factors varied from flight-to-flight due to variations in

aerosol composition and had average values of 1.44, 1.22, and 1.28 for volume, surface area, and effective radius, respectively. Note that this correction applies only to in situ size distributions at dry RH (less than 40 %).

After applying the aforementioned correction factors to the UHSAS measurements, we observed an overall improvement on the comparisons between the lidar retrievals and the UHSAS measurements. Volume and surface area concentrations still show underestimation when compared to the lidar retrievals, but they were both reduced to 71 %. Effective radius, on the other hand, improved to an average of -3 %, showing a slight overestimation with respect to the lidar retrievals. The in-situ size parameters displayed in Fig. 7 represent the corrected data.

The differences observed in volume and surface-area concentrations between lidar retrievals and in-situ measurements were first thought to be related to possible inlet issues in the P3B aircraft. Ziemba et al. (2013), however, concluded that particle loss due to the aerosol inlet was likely negligible after obtaining good correlation ( $r^2 = 0.88$ ) between in-situ extinction coefficient measurements from the P-3B at 532 nm and those obtained from HSRL also at 532 nm. This improved correlation (from  $r^2 = 0.81$ ) was obtained after the optical measurements obtained from the P-3B was corrected for the ambient RH using the measurements of hygroscopicity also obtained onboard. With this comparison Ziemba et al. (2013) found a liquid-water contribution to ambient extinction of up to 43 %.

After ruling out possible aircraft inlet issues, the most likely factor contributing to this difference observed is related to the aforementioned aerosol hydration processes. Condensation and evaporation from the particles surfaces during sampling are known to occur (Biswas et al., 1987; Leaitch and Isaac, 1991) which dries the aerosol during probing. The two nephelometers onboard the P-3B were utilized to calculate the changes in aerosol scattering due to hygroscopic growth, commonly expressed as  $f(\text{RH})$ . The hygroscopic growth, however, is determined by the relative increase in the diameter of the aerosol particles due to water uptake, commonly expressed by the growth factor  $g(\text{RH})$  which was not measured during DISCOVER-AQ. Therefore, corrections

## Aerosol optical and microphysical retrievals from a hybrid lidar dataset

P. Sawamura et al.

Title Page

Abstract

Introduction

Conclusions

References

Tables

Figures

⏪

⏩

◀

▶

Back

Close

Full Screen / Esc

Printer-friendly Version

Interactive Discussion

to the size distributions obtained by both UHSAS and LAS instruments with respect to water uptake were not performed.

Assuming that the size parameters obtained from the lidar retrievals are representative of particles in ambient humidity conditions and the ones obtained from the UHSAS on board P-3B are representative of particles in dry conditions, the ratio of volume concentration can be considered a first approximation for  $\bar{g}^3(\text{RH})$  and the ratio of surface-area concentrations an approximation for  $f(\text{RH})$ .  $\bar{g}(\text{RH})$  would be an average or effective growth factor for the entire range of diameters considered in the measurement. The ratio obtained in this study for the growth factor was  $\bar{g} = 1.75 \pm 0.17$ . The values for  $\bar{g}(\text{RH})$  reported in the literature for ammonium sulfate at 355 nm and 532 nm fall within the range 1.44–1.46 at RH = 80 % and 1.69–1.77 at RH = 90 % (Michel Flores et al., 2012; Gysel et al., 2002; Dinar et al., 2008; Sjogren et al., 2007). In terms of  $f(\text{RH})$ , the value obtained from the ratio between lidar and UHSAS surface-area concentration values was  $f(\text{RH}) = 2.16 \pm 0.34$ . Average values of  $f(\text{RH})$  for 11:00–13:00 EDT during DISCOVER-AQ (below 1 km of altitude) ranged between 1.28 and 1.91 (Ziemba et al., 2013).

We would like to emphasize the fact that the value obtained for  $\bar{g}(\text{RH})$  in this study can only be considered as a rough estimate of the hygroscopic growth factor. Also, the difference between the  $f(\text{RH})$  value obtained from this comparison and the values obtained by Ziemba et al. (2013) was marginal within 1 to 2 standard deviations. Aerosol hydration processes were clearly a major factor in the difference observed between the size parameters retrieved from lidar data and from the airborne in-situ measurements. However it remains inconclusive whether the difference was *solely* due to hydration processes. This matter will be subject to further investigation in future studies.

#### 4.4 Single-scattering albedo and complex index of refraction

The average single-scattering albedo value obtained from the lidar retrievals was  $\omega_0 = 0.95 \pm 0.02$  which agrees with the values reported in the literature for the Baltimore-Washington DC region at this particular time of the year. Dubovik et al. (2002)

## Aerosol optical and microphysical retrievals from a hybrid lidar dataset

P. Sawamura et al.

Title Page

Abstract

Introduction

Conclusions

References

Tables

Figures

⏪

⏩

◀

▶

Back

Close

Full Screen / Esc

Printer-friendly Version

Interactive Discussion



analyzed 8 years of worldwide AERONET retrievals and reported an average value of  $\omega_0(550\text{ nm}) \sim 0.97$  for the GSFC station between June and September.

Measurements obtained by the P-3B shows a systematic overestimation with respect to lidar retrievals with an average value of  $\omega_0 = 0.99 \pm 0.01$  for all spiral sites.

Another aircraft experiment conducted in the Mid-Atlantic region of the United States in July 1993, SCAR-A (Remer et al., 1997) reported a best estimate value similar to those obtained by the P-3B,  $\omega_0(450\text{ nm}) \sim 0.98\text{--}0.99$ . On the other hand, during another field campaign conducted in the Mid-Atlantic region on July 1996 (TARFOX), Hegg et al. (1997) found that aerosol absorption was a significant contributor to the total dry extinction measured ( $\sim 25\%$ ) which averaged over the vertical profiles in order to assess its contribution to the total optical depth resulted on an average  $\omega_0(550\text{ nm}) = 0.90$ . When hydration of aerosols was considered they estimated an upper limit of  $\omega_0(550\text{ nm}) = 0.94$ .

The  $m$  values obtained from our lidar retrievals also agree well with the values reported on the literature. Combining simultaneous in-situ size distribution profile measurements obtained onboard an aircraft with lidar aerosol backscatter and optical depth profiles, Redemann et al. (2001) obtained profiles of  $m$  for two case studies during TARFOX. Redemann et al. (2001) reported for the first case study values of  $1.33 - 0.0012i$  (0–250 m, RH = 80–100%),  $1.38 - 0.004i$  (250–1650 m, RH = 50–65%), and  $1.45 - 0.002i$  (1650–4030 m, RH = 30–50%). For the second case study it was found  $1.45 - 0.003i$  (150–1280 m, RH = 60–70%), and  $1.45 - 0.008i$  (1280–1980 m, RH = 40–60%) resulting in an average  $\text{Re}[m] = 1.41 \pm 0.06$  and  $\text{Im}[m] = 0.004 \pm 0.003$ , which agrees with the lidar average results. Dubovik et al. (2002) reported  $\text{Re}[m] = 1.40 \pm 0.01$  at GSFC (averaged over all wavelengths) from AERONET retrievals.

There are still many uncertainties on how light-absorbing aerosols affect our climate. The main uncertainties are related to their mixing state with other particles as well as with how light-absorbing particles respond to changes in ambient RH (Redemann et al., 2001; Haywood and Ramaswamy, 1998; Andreae, 2001). Bond et al. (2006) discusses how absorption due to light-absorbing carbon particles increases when they are mixed

## Aerosol optical and microphysical retrievals from a hybrid lidar dataset

P. Sawamura et al.

Title Page

Abstract

Introduction

Conclusions

References

Tables

Figures

⏪

⏩

◀

▶

Back

Close

Full Screen / Esc

Printer-friendly Version

Interactive Discussion



## Aerosol optical and microphysical retrievals from a hybrid lidar dataset

P. Sawamura et al.

Title Page

Abstract

Introduction

Conclusions

References

Tables

Figures

◀

▶

◀

▶

Back

Close

Full Screen / Esc

Printer-friendly Version

Interactive Discussion

were operating at UMBC during DISCOVER-AQ (Fig. 6). Airmass back-trajectories (not shown here) helped us to determine that some layers observed over Baltimore was likely to be residual smoke from the southern fires. As previously mentioned, this case did not present very high AOD values. Out of the cases analyzed, July 05 presented the smallest range of effective radius values from the lidar retrievals and this trend was consistent with the P-3B observations and AERONET retrievals as can be seen in Fig. 7. The retrievals obtained from the lidar data of the first overpass on July 05 (case A) showed a small value of  $\omega_0$  and a large value of  $\text{Im}[m]$  for the top layer (2.46 km –2.78 km). The values obtained,  $\omega_0 = 0.89 \pm 0.05$  and  $\text{Im}[m] = 0.013 \pm 0.005$  fall within the range of values observed for biomass burning cases presented by Dubovik et al. (2002):  $0.88 \leq \omega_0(440\text{ nm}) \leq 0.94$  and  $0.00093 \leq \text{Im}[m](440\text{ nm}) \leq 0.021$ . However, both retrievals of  $\omega_0$  and  $\text{Im}[m]$  for this particular case also showed large variation making it a less trustworthy retrieval. Therefore, definite conclusions on the retrieval sensitivity to capture the properties of a smoke layer could not be properly drawn in this case.  $\text{Re}[m]$  obtained from lidar for this case agreed with values obtained at UMBC and Padonia AERONET stations.

### 4.4.2 (22 July) Unusual size parameter case

The inversion code utilized for the lidar data can sometimes retrieve artificial bimodality in the size distributions. In order to identify those cases, the algorithm calculates the effective radius fine-to-total mode fraction ( $R_{\text{eff}}^{\text{fine}}/R_{\text{eff}}^{\text{total}}$ ) that varies from 0 to 1. This number can be used as a “quality flag”: the lower the number, the worse the retrieval. The cases from 22 July presented the lowest values of  $R_{\text{eff}}^{\text{fine}}/R_{\text{eff}}^{\text{total}}$  which translated into larger variation of the individual lidar retrievals causing the larger error bars observed in cases G and H from Fig. 7. It was later found that  $R_{\text{eff}}^{\text{fine}}/R_{\text{eff}}^{\text{total}}$  correlated with the depolarization ratio measurements obtained from the HSRL-1 lidar system. Figure 8 shows two distinct clusters with data from 22 July in red and the data from other dates in black.

The lidar inversion algorithm utilizes Mie theory for the calculations. Therefore, some retrieval sensitivity with respect to the presence of non-spherical aerosol particles is to be expected. The origin of the non-spherical particles observed in this particular case remains unknown.

## 5 Conclusions

For the first time we present daytime retrievals of optical and microphysical properties of aerosols derived from a hybrid multiwavelength lidar dataset. In particular, it was also the first study ever performed in the United States in which daytime multiwavelength lidar retrievals were obtained and compared to measurements obtained from airborne in-situ and AERONET retrievals.

Comparison of remote sensing retrievals with in-situ measurements of aerosols are usually technically challenging due to a number of factors. By definition, remote sensing instruments do not probe aerosols directly, measuring instead radiation that is scattered and/or emitted from them, while in-situ instruments usually collect aerosols either on filters or chambers in order to make measurements. If not properly characterized and calibrated, in-situ instruments may produce different results due to under-sampling as well as changes in temperature and relative humidity in the environment being sampled. Remote sensing instruments, on the other hand, present a different set of potential problems. The instruments must also be well calibrated and characterized, but in addition to that, the algorithms must be systematically validated to assure the quality of retrievals.

In this study we compared lidar retrievals of effective radius, volume and surface-area concentrations, single-scattering albedo and complex index of refraction with both AERONET level 1.5 and 2.0 retrievals which have been extensively studied and validated, and aircraft in-situ measurements (except  $m$ ).

During DISCOVER-AQ 2011 the lidar retrievals showed good agreement with AERONET retrievals for all parameters. The choice of an ALH of 1.5 km to convert

## Aerosol optical and microphysical retrievals from a hybrid lidar dataset

P. Sawamura et al.

Title Page

Abstract

Introduction

Conclusions

References

Tables

Figures

⏪

⏩

◀

▶

Back

Close

Full Screen / Esc

Printer-friendly Version

Interactive Discussion





## Aerosol optical and microphysical retrievals from a hybrid lidar dataset

P. Sawamura et al.

Title Page

Abstract

Introduction

Conclusions

References

Tables

Figures

◀

▶

◀

▶

Back

Close

Full Screen / Esc

Printer-friendly Version

Interactive Discussion

lidar systems that are capable of providing the  $3\beta + 2\alpha$  dataset. With the increasing number of collaborative projects and intensive field campaigns in which a number of different instruments are deployed in synergy, the possibilities of having multiple lidar systems deployed in proximity to each other increase, thus increasing the opportunities of characterizing the aerosols in different areas of the globe.

The methodology applied in this study was rather time-consuming and not practical for daily operational use. Nonetheless, the methodology can possibly be applied within the context of other field campaigns, hopefully with longer records of measurements for better assessment of more diverse atmospheric conditions as well as to test the sensitivity of the lidar retrievals especially with respect to the presence of light-absorbing aerosols.

NASA Langley Research Center (LaRC) recently developed the first airborne multi-wavelength HSRL instrument capable of providing a robust  $3\beta + 2\alpha$  dataset. HSRL-2 is an upgraded version of the airborne HSRL-1 system utilized in this study and it is capable of providing HSRL measurements at 355 and 532 nm, as well as elastic measurements at 1064 nm (Hostetler et al., 2013a, b). In addition to the new instrument NASA LaRC is also developing a new automated lidar inversion algorithm (Chemyakin et al., 2012) which will allow for more systematic validation of multiwavelength lidar retrievals.

*Acknowledgements.* This work was funded by grant NNX10AR38G (NASA DISCOVER-AQ).

## References

- Althausen, D., Müller, D., A., A., Wandinger, U., Hube, H., Clauder, E., and Zörner, S.: Scanning six-wavelength eleven-channel aerosol lidar, *J. Atmos. Ocean. Tech.*, 17, 1469–1482, 2000. 3123
- Andreae, M. O.: The dark side of aerosols, *Nature*, 409, 671–672, 2001. 3133
- Balis, D., Giannakaki, E., Müller, D., Amiridis, V., Kelektoglou, K., Rapsomanikis, S., and Bais, A.: Estimation of the microphysical aerosol properties over Thessaloniki, Greece, dur-

## Aerosol optical and microphysical retrievals from a hybrid lidar dataset

P. Sawamura et al.

Title Page

Abstract

Introduction

Conclusions

References

Tables

Figures

◀

▶

◀

▶

Back

Close

Full Screen / Esc

Printer-friendly Version

Interactive Discussion

ing SCOUT-O<sub>3</sub> campaign with the synergy of Raman lidar and Sun photometer data, *J. Geophys. Res.*, 115, D8, doi:10.1029/2009JD013088, 2010. 3117

Biswas, P., Jones, C. L., and Flagan, R. C.: Distortion of size distributions by condensation and evaporation in aerosol instruments, *Aerosol Sci. Tech.*, 1, 231–246, 1987. 3131

Bockmann, C., Mironova, I., and Muller, D.: Microphysical aerosol parameters from multiwavelength lidar, *J. Opt. Soc. Am. A*, 22, 518–528, 2005. 3116, 3118, 3123

Bohren, C. F. and Huffman, D. R.: Absorption and scattering of light by small particles, Wiley Science Paperback Series, Wiley, 1983. 3123

Bond, T. C., Habib, G., and Bergstrom, R. W.: Limitations in the enhancement of visible light absorption due to mixing state, *J. Geophys. Res.*, 111, D20, doi:10.1029/2006JD007315, 2006. 3133

Bösenberg, J., Matthias, V., Amodeo, A., Amoiridis, V., Ansmann, A., Baldasano, J. M., Balin, I., Balis, D., Böckmann, C., Boselli, A., Carlsson, G., Chaikovsky, A., Chourdakis, G., Comerón, A., Tomasi, F., Eixmann, R., Freudenthaler, V., Giehl, H., Grigorov, I., Hågård, A., Iarlori, M., Kirsche, A., Kolarov, G., Komguem, L., Kreipl, S., Kumpf, W., Larchevêque, G., Linné, H., Matthey, R., Mattis, I., Mekler, A., Mironova, I., Mitev, V., Mona, L., Müller, D., Music, S., Nickovic, S., Pandolfi, M., Papayannis, A., Pappalardo, G., Pelon, H., Pérez, C., Perrone, R. M., Persson, R., Resendes, D. P., Rizi, V., Rocadenbosch, F., Rodrigues, J. A., Sauvage, L., Schneidenbach, L., Schumacher, R., Shcherbakov, V., Simeonov, V., Sobolewski, P., Spinelli, N., Stachlewska, I., Stoyanov, D., Trickl, T., Tsaknakis, G., Vaughan, G., Wandinger, U., Wang, X., Wiegner, M., Zavrtnik, M., and Zerefos, C.: EARLINET: A European Aerosol Research Lidar Network to Establish an Aerosol Climatology, Tech. rep., Max Planck Institute for Meteorology, 2003. 3115

Chemyakin, E., Kolgotin, A., Romanov, A., and Müller, D.: Automated, unsupervised inversion of multiwavelength Raman lidar data: Statistical analysis of microphysical parameters, in: Proceedings of the 26th International Laser Radar Conference, Porto Heli, Greece, 2012, S1P–49, 2012. 3138

Comer, J.: UMBC Elastic Backscatter Lidar Facility (ELF): subvisible cirrus cloud and aerosol measurements during ABOVE 2002, Master's thesis, University of Maryland, Baltimore County, 2003. 3121

Dinar, E., Abo Riziq, A., Spindler, C., Erlick, C., Kiss, G., and Rudich, Y.: The complex refractive index of atmospheric and model humic-like substances (HULIS) retrieved by a cavity ring down aerosol spectrometer (CRD-AS), *Faraday Discuss.*, 137, 279–295, 2008. 3132



## Aerosol optical and microphysical retrievals from a hybrid lidar dataset

P. Sawamura et al.

Title Page

Abstract

Introduction

Conclusions

References

Tables

Figures

◀

▶

◀

▶

Back

Close

Full Screen / Esc

Printer-friendly Version

Interactive Discussion

termining the relationship between satellite retrieved column AOD, extinction profiles and surface  $PM_{2.5}$ , in: Proceedings of 26th International Laser Radar Conference, Porto Heli, Greece, 2012. 3118

Holben, B. N., Eck, T. F., Slutsker, I., Tanré, D., Buis, J. P., Setzer, A., Vermote, E., Reagan, J. A., Kaufman, Y. J., Nakajima, T., Lavenu, F., Jankowiak, I., and Smirnov, A.: AERONET – a federated instrument network and data archive for aerosol characterization, *Remote Sens. Environ.*, 66, 1–16, 1998. 3127

Holben, B. N., Eck, T. F., Slutsker, I., Smirnov, A., Sinyuk, A., Schafer, J., Giles, D., and Dubovik, O.: AERONET's Version 2.0 quality assurance criteria, in: Proc. SPIE 6408, Remote Sensing of the Atmosphere and Clouds, 64080Q, 64080 pp.Q–64080Q–14, 2006. 3128

Holben, B. N., Eck, T., Schafer, J., Giles, D., and Sorokin, M.: Distributed Regional Aerosol Gridded Observation Networks (DRAGON) White Paper, available at: [http://aeronet.gsfc.nasa.gov/new\\_web/Documents/DRAGON\\_White\\_Paper\\_A\\_system\\_of\\_experiment.pdf](http://aeronet.gsfc.nasa.gov/new_web/Documents/DRAGON_White_Paper_A_system_of_experiment.pdf) (last access: 19 March 2014), 2011. 3127

Hostetler, C. A., Ferrare, R., Hair, J., Cook, A., Harper, D., Rogers, R. R., Müller, D., Burton, S., Obland, M. D., Scarino, A. J., Schmid, B., Fast, J., Berg, L., Flynn, C., Cairns, B., Russell, P., Redemann, J., and Shinozuka, Y.: Airborne Multi-wavelength High Spectral Resolution Lidar Observations and Applications from TCAP, available at: <http://asr.science.energy.gov/meetings/stm/posters/view?id=797> (last access: 19 March 2014), 2013a. 3138

Hostetler, C. A., Ferrare, R., Hair, J., Cook, A., Harper, D., Mack, T., Hare, R., Cleckner, C., Rogers, R. R., Müller, D., Chemyakin, E., Burton, S., Scarino, A. J., Obland, M. D., Chand, D., Tomlinson, J., Cairns, B., Russell, P., Redemann, J., Shinozuka, Y., Schmid, B., Fast, J., Berg, L., and Flynn, C.: Airborne Multi-wavelength High Spectral Resolution Lidar Observations and Applications from TCAP, available at: <http://asr.science.energy.gov/meetings/stm/2013/presentations/Ferrare-TCAP-HSRL-03192013.pdf> (last access: 19 March 2014), 2013b. 3138

Jacobson, M.: Air Pollution and Global Warming: History, Science, and Solutions, Cambridge University Press, 2012. 3115

Leaich, W. and Isaac, G.: Tropospheric aerosol size distributions from 1982 to 1988 over eastern North America, *Atmos. Environ. A-Gen.*, 25, 601–619, 1991. 3131

Michel Flores, J., Bar-Or, R. Z., Bluvshstein, N., Abo-Riziq, A., Kostinski, A., Borrmann, S., Koren, I., Koren, I., and Rudich, Y.: Absorbing aerosols at high relative humidity: linking hygro-

**Aerosol optical and  
microphysical  
retrievals from  
a hybrid lidar dataset**

P. Sawamura et al.

[Title Page](#)[Abstract](#)[Introduction](#)[Conclusions](#)[References](#)[Tables](#)[Figures](#)[⏪](#)[⏩](#)[◀](#)[▶](#)[Back](#)[Close](#)[Full Screen / Esc](#)[Printer-friendly Version](#)[Interactive Discussion](#)

scopic growth to optical properties, *Atmos. Chem. Phys.*, 12, 5511–5521, doi:10.5194/acp-12-5511-2012, 2012. 3132

Mie, G.: Beiträge zur Optik trüber Medien, speziell kolloidaler Metallösungen, *Ann. Phys.*, 25, 377–445, 1908. 3123

5 Müller, D., Wandinger, U., Althausen, D., Mattis, I., and Ansmann, A.: Retrieval of physical particle properties from lidar observations of extinction and backscatter at multiple wavelengths, *Appl. Optics*, 37, 2260–2263, 1998. 3116, 3117, 3122, 3123

Müller, D., Wandinger, U., and Ansmann, A.: Microphysical particle parameters from extinction and backscatter lidar data by inversion with regularization: Theory, *Appl. Optics*, 38, 2346–2357, 1999a. 3116, 3123, 3124

10 Müller, D., Wandinger, U., and Ansmann, A.: Microphysical particle parameters from extinction and backscatter lidar data by inversion with regularization: simulation, *Appl. Optics*, 38, 2358–2368, 1999b. 3116, 3123

15 Müller, D., Wagner, F., Wandinger, U., Ansmann, A., Wendisch, M., Althausen, D., and von Hoyningen-Huene, W.: Microphysical particle parameters from extinction and backscatter lidar data by inversion with regularization: experiment, *Appl. Optics*, 39, 1879–1892, 2000. 3123

20 Müller, D., Wandinger, U., Althausen, D., and Fiebig, M.: Comprehensive particle characterization from three-wavelength Raman-lidar observations: case study, *Appl. Optics*, 40, 4863–4869, 2001. 3117, 3123

Müller, D., Franke, K., Ansmann, A., Althausen, D., and Wagner, F.: Indo-Asian pollution during INDOEX: Microphysical particle properties and single-scattering albedo inferred from multiwavelength lidar observations, *J. Geophys. Res.*, 108, D19, doi:10.1029/2003JD003538, 2003. 3117

25 Müller, D., Kolgotin, A., Mattis, I., Petzold, A., and Stohl, A.: Vertical profiles of microphysical particle properties derived from inversion with two-dimensional regularization of multiwavelength Raman lidar data: Experiment, *Appl. Optics*, 50, 2069–2079, 2011. 3117

30 Noh, Y. M., Müller, D., Shin, D. H., Lee, H., Jung, J., Lee, K. H., Cribb, M., Li, Z., and Kim, Y. J.: Optical and microphysical properties of severe haze and smoke aerosol measured by integrated remote sensing techniques in Gwangju, Korea, *Atmos. Environ.*, 43, 879–888, 2009. 3117



**Aerosol optical and  
microphysical  
retrievals from  
a hybrid lidar dataset**

P. Sawamura et al.

[Title Page](#)[Abstract](#)[Introduction](#)[Conclusions](#)[References](#)[Tables](#)[Figures](#)[⏪](#)[⏩](#)[◀](#)[▶](#)[Back](#)[Close](#)[Full Screen / Esc](#)[Printer-friendly Version](#)[Interactive Discussion](#)

Veselovskii, I., Kolgotin, A., Griaznov, V., Müller, D., Franke, K., and Whiteman, D. N.: Inversion of multiwavelength Raman lidar data for retrieval of bimodal aerosol size distribution, *Appl. Optics*, 43, 1180–1195, 2004. 3118

Veselovskii, I., Whiteman, D. N., Kolgotin, A., Andrews, E., and Korenskii, M.: Demonstration of aerosol property profiling by multiwavelength lidar under varying relative humidity conditions, *J. Atmos. Ocean. Tech.*, 26, 1543–1557, 2009. 3116, 3117

Veselovskii, I., Dubovik, O., Kolgotin, A., Korenskiy, M., Whiteman, D. N., Allakhverdiev, K., and Huseyinoglu, F.: Linear estimation of particle bulk parameters from multi-wavelength lidar measurements, *Atmos. Meas. Tech.*, 5, 1135–1145, doi:10.5194/amt-5-1135-2012, 2012a. 3117

Veselovskii, I., Kolgotin, A., Korenskiy, M., Whiteman, D., Dubovik, O., and Volkov, N.: Linear estimation of time series of bulk particle parameters from multiwavelength lidar measurements, in: *Proceedings of the 26th International Laser Radar Conference, Porto Heli, Greece, 2012, S3P–15, 2012b.* 3125

Veselovskii, I., Whiteman, D. N., Kolgotin, A., Korenskiy, M., and Perez-Ramirez, D.: Retrieval of height-temporal distributions of particle parameters from multiwavelength lidar measurements during DISCOVER-AQ 2011 campaign, in: *Proceedings of the 26th International Laser Radar Conference, Porto Heli, Greece, 2012, S3O–14, 2012c.* 3117, 3125

Wagner, J., Ansmann, A., Wandinger, U., Seifert, P., Schwarz, A., Tesche, M., Chaikovskiy, A., and Dubovik, O.: Evaluation of the Lidar/Radiometer Inversion Code (LIRIC) to determine microphysical properties of volcanic and desert dust, *Atmos. Meas. Tech.*, 6, 1707–1724, doi:10.5194/amt-6-1707-2013, 2013. 3119

Wandinger, U., Müller, D., Böckmann, C., Althausen, D., Matthias, V., Bösenberg, J., Weiß, Fiebig, M., Wendisch, M., Stohl, A., and Ansmann, A.: Optical and microphysical characterization of biomass-burning and industrial-pollution aerosols from multiwavelength lidar and aircraft measurements, *J. Geophys. Res.*, 107, D21, doi:10.1029/2000JD000202, 2002. 3116, 3117

Weitkamp, C.: *Lidar: Range-resolved Optical Remote Sensing of the Atmosphere*, Springer Series in Optical Sciences, Springer, 2005. 3124, 3125

Welton, E. J., Campbell, J. R., Spinhirne, J. D., and Scott, V. S.: Global monitoring of clouds and aerosols using a network of micro-pulse lidar systems, in: *Lidar Remote Sensing for Industry and Environmental Monitoring*, edited by: Singh, U. N., Itabe, T., and Sugimoto, N., vol. 4153 of *Proc. SPIE*, 151–158, 2001. 3115

Ziamba, L. D., Lee Thornhill, K., Ferrare, R., Barrick, J., Beyersdorf, A. J., Chen, G., Crumeyrolle, S. N., Hair, J., Hostetler, C., Hudgins, C., Obland, M., Rogers, R., Scarino, A. J., Winstead, E. L., and Anderson, B. E.: Airborne observations of aerosol extinction by in situ and remote-sensing techniques: Evaluation of particle hygroscopicity, *Geophys. Res. Lett.*, 40, 417–422, 2013. 3127, 3131, 3132

5

# AMTD

7, 3113–3157, 2014

## Aerosol optical and microphysical retrievals from a hybrid lidar dataset

P. Sawamura et al.

Title Page

Abstract

Introduction

Conclusions

References

Tables

Figures



Back

Close

Full Screen / Esc

Printer-friendly Version

Interactive Discussion





## Aerosol optical and microphysical retrievals from a hybrid lidar dataset

P. Sawamura et al.

**Table 2.** Average of results obtained from lidar retrievals (i.e.  $3\beta + 2\alpha$ ), in-situ measurements from P-3B flights, and AERONET retrievals of effective radius ( $R_{\text{eff}}$ ), volume and surface-area concentrations, and single scattering albedo. Real and imaginary parts of the complex index of refraction were compared to AERONET only. Maximum aerosol layer height (AHL) was assumed as 1.5 km in order to convert AERONET volume and surface-area concentrations from per unit area to per unit volume. Mean values from AERONET are presented for three different averaging subsets. Number of data points for each subset is presented between parentheses for size and optical related parameters.

	$R_{\text{eff}}$ [ $\mu\text{m}$ ]	Vol. Conc. [ $\mu\text{m}^3 \text{cm}^{-3}$ ]	S-Area Conc. [ $\mu\text{m}^2 \text{cm}^{-3}$ ]	$\omega_0$	Re( $m$ )	Im( $m$ )
$3\beta + 2\alpha$	$0.18 \pm 0.05$	$45 \pm 23$	$821 \pm 369$	$0.95 \pm 0.02$	$1.39 \pm 0.03$	$0.005 \pm 0.002$
P-3B Beltsville	$0.13 \pm 0.02$	$10 \pm 5$	$224 \pm 74$	$0.99 \pm 0.01$	N/A	N/A
P-3B Essex	$0.13 \pm 0.02$	$8 \pm 4$	$181 \pm 65$	$0.99 \pm 0.01$	N/A	N/A
P-3B Padonia	$0.14 \pm 0.02$	$8 \pm 3$	$178 \pm 57$	$0.99 \pm 0.01$	N/A	N/A
AERO UMBC <sup>a</sup>	$0.17 \pm 0.02$ (11)	$54 \pm 20$	$963 \pm 350$	$0.94 \pm 0.03$ (11)	$1.41 \pm 0.03$	$0.007 \pm 0.004$
AERO UMBC <sup>b</sup>	$0.17 \pm 0.01$ (8)	$51 \pm 21$	$925 \pm 377$	$0.94 \pm 0.02$ (5)	$1.40 \pm 0.03$	$0.007 \pm 0.003$
AERO UMBC <sup>c</sup>	$0.16 \pm 0.02$ (51)	$31 \pm 19$	$580 \pm 311$	$0.94 \pm 0.02$ (15)	$1.41 \pm 0.03$	$0.008 \pm 0.003$
AERO GSFC <sup>a</sup>	$0.18 \pm 0.03$ (10)	$51 \pm 15$	$871 \pm 297$	$0.98 \pm 0.01$ (10)	$1.40 \pm 0.04$	$0.003 \pm 0.002$
AERO GSFC <sup>b</sup>	$0.19 \pm 0.03$ (4)	$47 \pm 19$	$747 \pm 364$	$0.98 \pm 0.01$ (3)	$1.41 \pm 0.04$	$0.003 \pm 0.002$
AERO GSFC <sup>c</sup>	$0.16 \pm 0.03$ (53)	$33 \pm 21$	$603 \pm 333$	$0.98 \pm 0.01$ (20)	$1.40 \pm 0.03$	$0.003 \pm 0.002$
AERO Essex <sup>a</sup>	$0.18 \pm 0.02$ (10)	$47 \pm 16$	$783 \pm 259$	$0.97 \pm 0.02$ (10)	$1.43 \pm 0.02$	$0.004 \pm 0.003$
AERO Essex <sup>b</sup>	$0.18 \pm 0.02$ (4)	$45 \pm 21$	$761 \pm 323$	$0.96 \pm 0.03$ (2)	$1.41 \pm 0.03$	$0.005 \pm 0.005$
AERO Essex <sup>c</sup>	$0.16 \pm 0.03$ (45)	$27 \pm 21$	$471 \pm 345$	$0.97 \pm 0.02$ (13)	$1.42 \pm 0.04$	$0.004 \pm 0.002$
AERO Beltsville <sup>a</sup>	$0.17 \pm 0.02$ (4)	$40 \pm 13$	$673 \pm 250$	$0.98 \pm 0.02$ (4)	$1.42 \pm 0.03$	$0.003 \pm 0.002$
AERO Beltsville <sup>b</sup>	$0.17 \pm 0.01$ (2)	$40 \pm 20$	$732 \pm 375$	N/A	N/A	N/A
AERO Beltsville <sup>c</sup>	$0.16 \pm 0.02$ (70)	$27 \pm 21$	$487 \pm 315$	$0.97 \pm 0.02$ (10)	$1.40 \pm 0.03$	$0.003 \pm 0.002$
AERO Padonia <sup>a</sup>	$0.18 \pm 0.02$ (10)	$57 \pm 27$	$968 \pm 479$	$0.95 \pm 0.02$ (10)	$1.41 \pm 0.03$	$0.006 \pm 0.003$

<sup>a</sup> Level 1.5: Data subset used to compare with lidar retrievals listed in Table 1.

<sup>b</sup> Level 2.0: Data subset used to compare with lidar retrievals listed in Table 1 (less data points).

<sup>c</sup> Level 2.0: Average of July 2011 data.

Title Page

Abstract Introduction

Conclusions References

Tables Figures

◀ ▶

◀ ▶

Back Close

Full Screen / Esc

Printer-friendly Version

Interactive Discussion



## Aerosol optical and microphysical retrievals from a hybrid lidar dataset

P. Sawamura et al.

**Table 4.** July mean values of single scattering albedo  $\omega_0$  for different aerosol loadings and different quality levels for all AERONET/DRAGON stations considered in this study.

	$\omega_0$ at 532 nm			
	$0 \leq \tau_{440} \leq 0.2$ Level 1.5	$0.2 \leq \tau_{440} \leq 0.4$ Level 1.5	$\tau_{440} \geq 0.4$ Level 1.5	$\tau_{440} \geq 0.4$ Level 2.0
Beltsville	$0.93 \pm 0.05$ (27)	$0.96 \pm 0.03$ (21)	$0.97 \pm 0.02$ (22)	$0.97 \pm 0.02$ (10)
Essex	$0.96 \pm 0.03$ (38)	$0.97 \pm 0.02$ (28)	$0.97 \pm 0.05$ (36)	$0.97 \pm 0.02$ (13)
GSFC	$0.96 \pm 0.03$ (49)	$0.96 \pm 0.02$ (29)	$0.98 \pm 0.01$ (43)	$0.98 \pm 0.01$ (20)
UMBC	$0.84 \pm 0.07$ (37)	$0.90 \pm 0.04$ (35)	$0.94 \pm 0.03$ (32)	$0.94 \pm 0.02$ (15)
Padonia	$0.84 \pm 0.05$ (41)	$0.92 \pm 0.06$ (50)	$0.97 \pm 0.02$ (37)	N/A

[Title Page](#)
[Abstract](#)
[Introduction](#)
[Conclusions](#)
[References](#)
[Tables](#)
[Figures](#)
[Back](#)
[Close](#)
[Full Screen / Esc](#)
[Printer-friendly Version](#)
[Interactive Discussion](#)

**Aerosol optical and  
microphysical  
retrievals from  
a hybrid lidar dataset**

P. Sawamura et al.

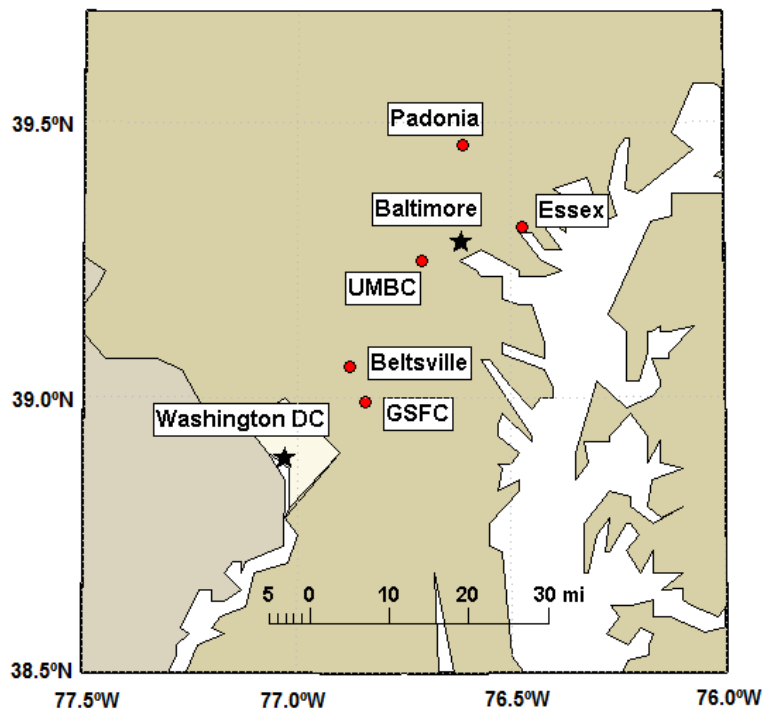


**Fig. 1.** Map of Baltimore-Washington DC region with the locations considered for the lidar retrievals comparison to AERONET retrievals and in-situ airborne measurements during DISCOVER-AQ.

Title Page

Abstract

Introduction

Conclusions

References

Tables

Figures

◀

▶

◀

▶

Back

Close

Full Screen / Esc

Printer-friendly Version

Interactive Discussion

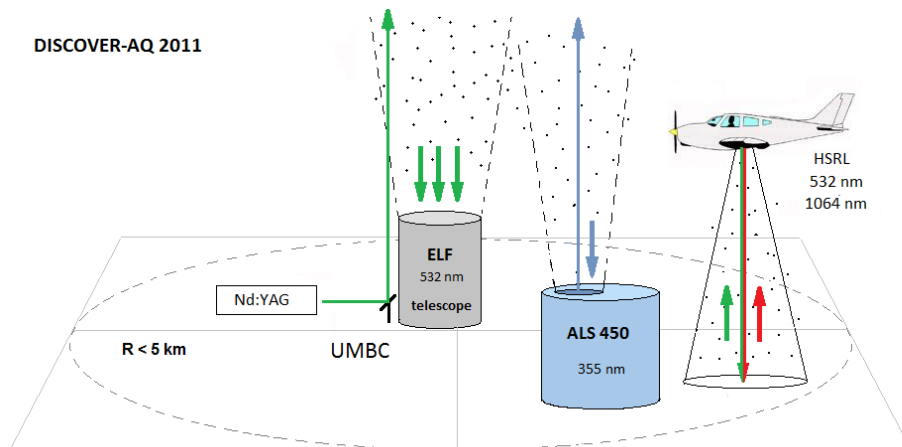


**Fig. 2.** Setup of airborne and ground-based instruments at UMBC during DISCOVER-AQ 2011. A maximum radius of 5 km was considered to construct the hybrid multiwavelength lidar dataset using HSRL and ALS-450 data.

## Aerosol optical and microphysical retrievals from a hybrid lidar dataset

P. Sawamura et al.

Title Page

Abstract

Introduction

Conclusions

References

Tables

Figures

◀

▶

◀

▶

Back

Close

Full Screen / Esc

Printer-friendly Version

Interactive Discussion



## Aerosol optical and microphysical retrievals from a hybrid lidar dataset

P. Sawamura et al.

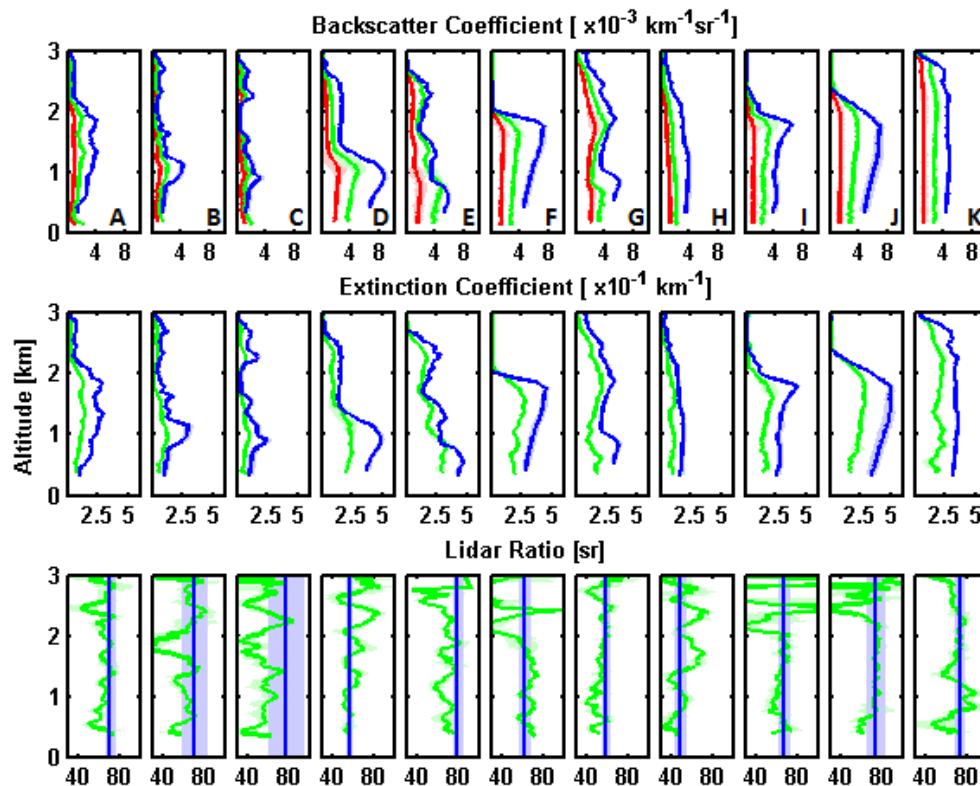


**Fig. 4.**  $3\beta + 2\alpha$  and lidar ratio values obtained from the hybrid multiwavelength lidar dataset. Green and red lines are airborne profiles at 532 nm (HSRL) and 1064 nm (elastic), respectively. Blue lines are from ground-based elastic lidar at 355 nm. Letters correspond to each case analyzed which are listed in detail in Table 1.

## Aerosol optical and microphysical retrievals from a hybrid lidar dataset

P. Sawamura et al.

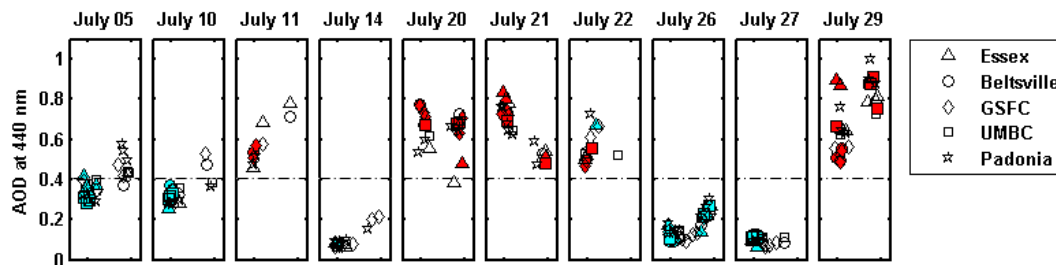


**Fig. 5.** Aerosol optical depth (AOD) at 440 nm obtained from AERONET stations at Essex, Beltsville, Goddard Space Flight Center (GSFC), UMBC and Padonia during all 10 days during DISCOVER-AQ in which there synergistic measurements among UC-12, P-3B and the ground-based lidar at UMBC. Empty symbols represent available level 1.5 retrievals of size-related products, single scattering albedo and complex index of refraction. Cyan-filled symbols represent available level 2.0 retrievals of only size-related products. Red-filled symbols represent available level 2.0 retrievals size-related products, single scattering albedo, and complex index of refraction. X axis of each window represents a day of AERONET measurement: sunrise to sunset.

Title Page

Abstract

Introduction

Conclusions

References

Tables

Figures

◀

▶

◀

▶

Back

Close

Full Screen / Esc

Printer-friendly Version

Interactive Discussion

**Aerosol optical and  
microphysical  
retrievals from  
a hybrid lidar dataset**

P. Sawamura et al.

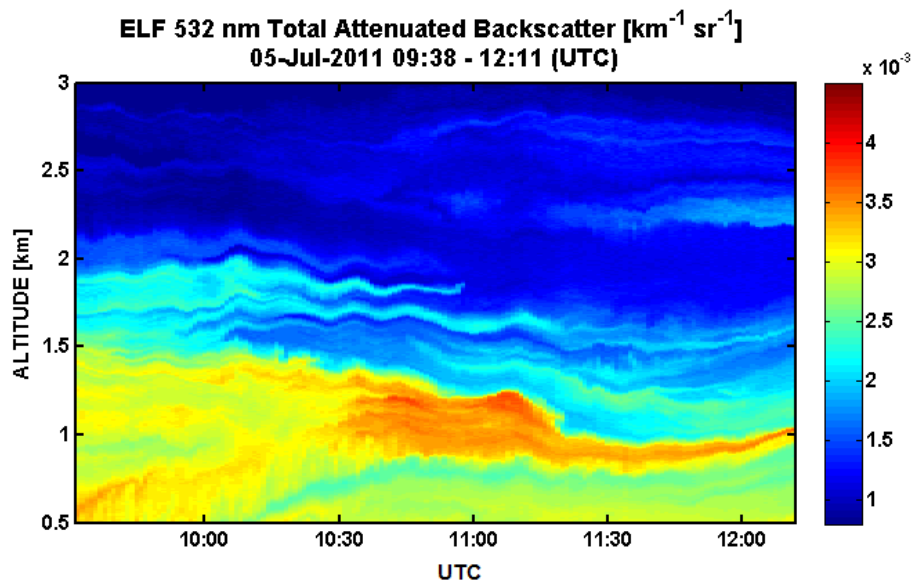


**Fig. 6.** Total attenuated backscatter coefficient cross-section obtained with elastic lidar (ELF) at 532 nm at UMBC on 5 July. Long range transport of smoke from fires occurring in the South-eastern portion of the US was observed.

Title Page

Abstract

Introduction

Conclusions

References

Tables

Figures

◀

▶

◀

▶

Back

Close

Full Screen / Esc

Printer-friendly Version

Interactive Discussion

## Aerosol optical and microphysical retrievals from a hybrid lidar dataset

P. Sawamura et al.

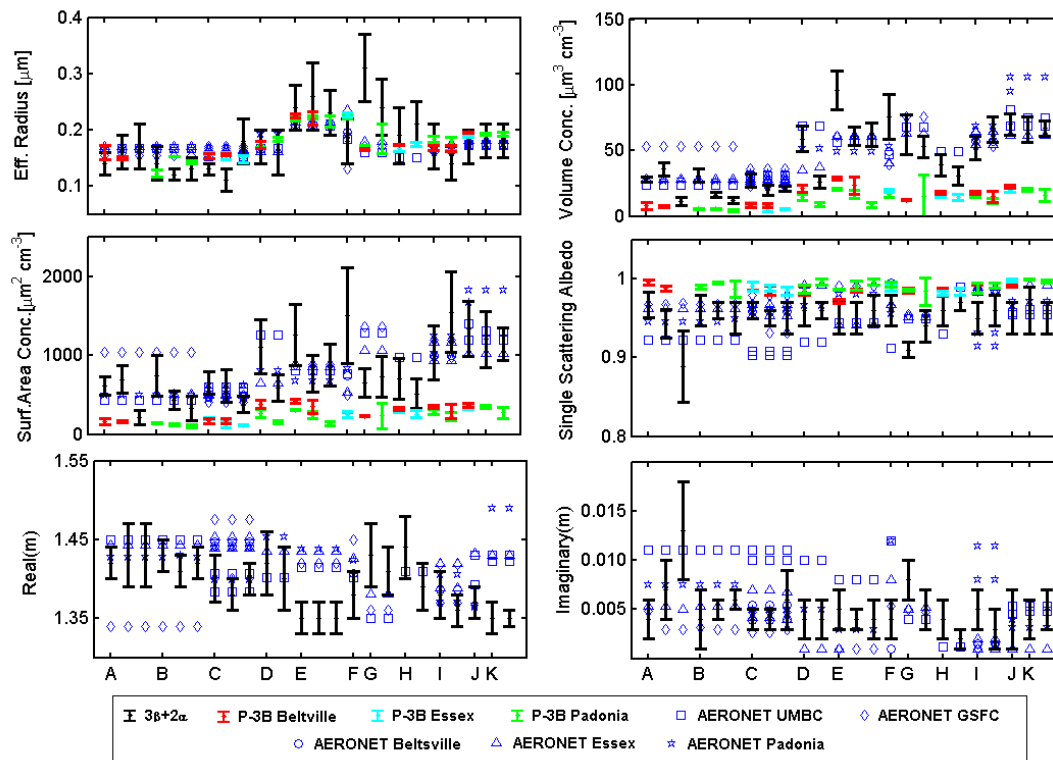


**Fig. 7.** Results of effective radius, volume and surface-area concentrations, single scattering albedo and complex index of refraction obtained from inversion of the hybrid multiwavelength lidar dataset ( $3\beta + 2\alpha$ ), from AERONET inversions and from in-situ measurements obtained by the P-3B aircraft (at dry conditions).

**Aerosol optical and  
microphysical  
retrievals from  
a hybrid lidar dataset**

P. Sawamura et al.

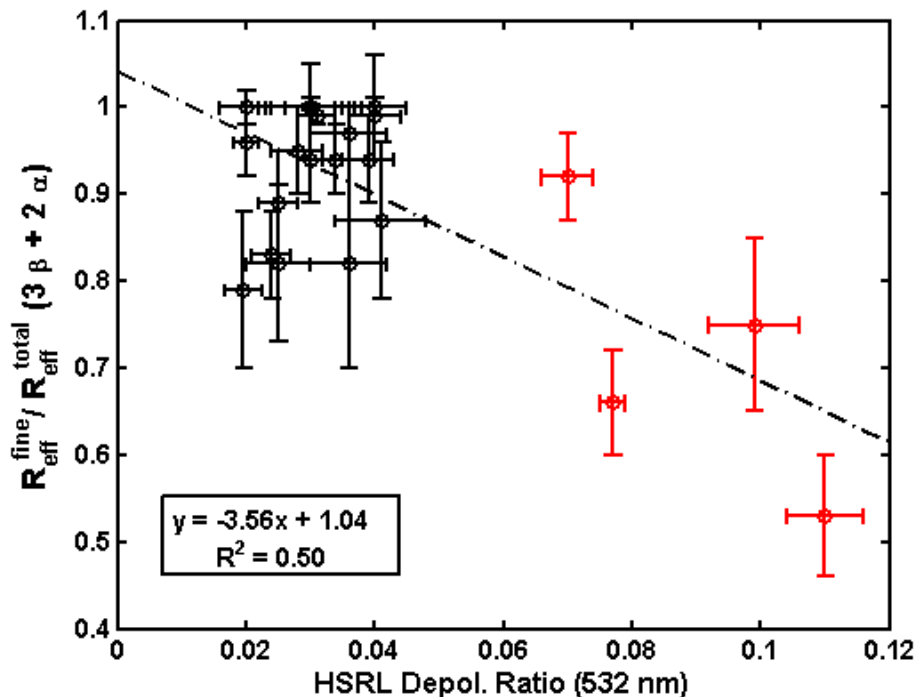


**Fig. 8.** Effective radius fine-to-total mode fraction from lidar retrievals vs. total (volume) depolarization ratio at 532 nm retrieved from HSRL-1. All cases and layers are displayed. Red circles represent 22 July data.

Title Page

Abstract

Introduction

Conclusions

References

Tables

Figures

◀

▶

◀

▶

Back

Close

Full Screen / Esc

Printer-friendly Version

Interactive Discussion